Crack-Resistance Behavior of Polypropylene Copolymers

WOLFGANG GRELLMANN,[1] SABINE SEIDLER,[2] KERSTIN JUNG,[1] INES KOTTER[1]

[1] Department of Engineering Science, Martin-Luther University Halle-Wittenberg, D-06099 Halle/Saale, Germany

[2] Vienna University of Technology, Department of Materials Science and Testing, A-1040 Wien, Austria

Received 11 May 1999; accepted 12 September 1999

ABSTRACT: Two heterophasic reactor-grade propylene–ethylene copolymers (RAHECO®) were diluted with propylene–ethylene random copolymers to obtain materials with constant EPR/PE-particle diameter but various interparticle distances. According to the results of instrumented impact tests, brittle-to-tough transitions were found at different temperatures. The critical interparticle distances shift linearly over the observed range of temperature. Critical interparticle distances could be determined not only in the region of predominantly unstable crack growth but also in the region of predominantly stable crack growth. © 2001 John Wiley & Sons, Inc. J Appl Polym Sci 79: 2317–2325, 2001

Key words: polypropylene; fracture toughness; morphology; interparticle distance; stability assessment diagram; crack resistance curve; brittle-to-tough transition

INTRODUCTION

Polypropylene is characterized by a poor low-temperature impact behavior because of its relatively high glass transition temperature. Modifying by elastomer particles improves the fracture toughness. PP/EPR blends can be more effectively produced by polymerization of the monomers directly in the reactor. In this way, it is possible to get materials with distinctive, well-dispersed morphologies.

The size, shape, and spatial packing of elastomer particles varied by manufacturing and processing conditions are important parameters in controlling the micromechanical and mechanical behavior of PP/EPR blends and copolymers.

Wu[1] explained that a critical interparticle distance or critical matrix ligament thickness exists, below which the notched Izod impact strength of nylon blends increases rapidly. He defined this increase of notched Izod impact strength as brittle-to-tough transition, and the critical value of interparticle distance, A_c, as a specific parameter of the material. Borggreve[2] and Margolina[3] showed that the critical interparticle distance in nylon blends is strongly affected by rate, method of loading, and test temperature. They proved an approximately linear dependence of the critical interparticle distance on temperature.

The aforementioned theories about the nature of transition from brittle to tough are based on conventional notched impact strengths. In conventional impact tests specimen fracture must occur; otherwise, no values can be determined. That means only a part of stable crack growth is included in the "notched impact strength." On the basis of the conventional notched impact strength it is not possible to separate the stable and the unstable part of the crack growth process. There is a possibility that the controversial discussion about the nature of transition from brittle to ductile mode of fracture is due to the fact that the crack growth behavior is unknown.

Fracture mechanics tests for unstable crack growth as well as stable crack growth are de-

Correspondence to: W. Grellmann.
Contract grant sponsor: DFG.

Journal of Applied Polymer Science, Vol. 79, 2317–2325 (2001)

scribed. By means of the application of approximate methods it is also possible to get fracture mechanics values over the whole range of temperature and experimental conditions even if no unstable crack growth occurs.

EXPERIMENTAL

Fracture Mechanics Characterization

A Charpy impact tester with 4 J work capacity was used and load (F)–deflection (f) curves were recorded.[4,5] Semiconductor strain gauges were used to measure the impact load. The deflection was recorded with the help of a photo-optical system. The dimensions of the injection moulded single edge notched bend (SENB) specimens were length $L = 80$ mm, width $W = 10$ mm, and thickness $B = 4$ mm. The specimens were notched with a razor blade (notch tip radius = 0.2 μm). For these specimens the test conditions were optimized by simulating specimen loading by a finite element method.[6] Experimental parameters were initial crack length $a = 2$ mm ($a/W = 0.2$), support span $s = 40$ mm ($s/W = 4$), and pendulum hammer speed $\nu_H = 1.5$ ms^{-1}. With regard to the elastic-plastic material behavior of polymers for the determining of J-integral values, the evaluation method by Sumpter and Turner[7] is especially suited for assessing the toughness behavior. A separation of the specimen deformation energy of test specimen, A_G, in an elastic share, A_{el}, and a plastic share, A_{pl}, is necessary for the calculation of J-integral values to correspond to this method. Therefore, eq. (1) was used for the determination of crack resistance values against unstable crack growth

$$J_{Qd}^{ST} = \eta_{el}\frac{A_{el}}{B(W-a)} + \eta_{pl}\frac{A_{pl}}{B(W-a)}\frac{W-a_{eff}}{W-a} \quad (1)$$

where

$$\eta_{el} = \frac{2F_{GY}s^2(W-a)}{f_{GY}E_dBW^3} f(a/W)(1-\nu^2) \quad (2)$$

and

$$\eta_{pl} = 2 - \frac{(1-a/W)(0.892-4.476a/W)}{1.125+0.892a/W-2.238(a/W)^2} \quad (3)$$

where F_{GY} and f_{GY} are the load and deflection at the transition point from elastic to elastic-plastic material behavior; and E_d is the dynamic flexural modulus according to ISO 178.[8]

If the deformation process is characterized by dominant stable crack growth, an additional energy part occurs—the so-called "crack propagation energy," A_R—and fracture mechanics values against stable crack growth must be used for toughness characterization. The evaluation of these fracture mechanics values requires the determination of crack resistance (J_R) curves. One well established method to determine J_R curves is the stop-block technique,[9] where the input pendulum hammer speed is constant. Different amounts of stable crack growth are produced by varying the limitation of deflection.

Whereas the specimen geometry is the same as in the unstable region, the optimized test conditions change. The initial crack length amounts to 4.5 mm ($a/W = 0.45$). For the determination of crack resistance curves, the usual multiple specimen technique was applied. The experimental results in refs. 10 and 11 show the necessity of the load separation. Therefore, the calculation of J-integral values against stable crack growth followed eq. (4).

$$J = \eta_{el}\frac{A_{el}}{B(W-a)} + \eta_{pl}\frac{A_{pl}}{B(W-a)} \times \left\{1 - \frac{(0.75\eta_{el}-1)\Delta a}{W-a}\right\} \quad (4)$$

The constructed J_R curves enable the quantification of the critical value at the onset of stable crack initiation, for instance, the technical crack initiation value, $J_{0.2}$, and also the determination of materials resistance against stable crack growth with the tearing modulus, T_J.

$$T_J = \frac{dJ}{d(\Delta a)}\frac{E_d}{\sigma_d^2} \quad (5)$$

By using the $J - T_J$-stability-assessment diagrams[12] (see Fig. 1) it is possible to determine unstable crack toughness values, if no unstable crack growth occurs under the experimental test conditions chosen. Figure 1 shows the implementation of a graphical transformation of a crack resistance curve in a $J - T_J$-stability-assessment diagram as an example of a typical PP material.

According to a suggestion of Paris and Johnson[12] the intersection between a load line and the J_R-curve can be determined following eq. (6).

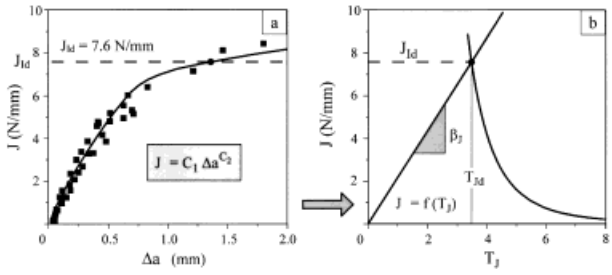

Figure 1 Graphical transformation of crack resistance curve (a) in a $J - T_J$-stability-assessment diagram (b) using unstable J_{Id}-parameter; β_J is characterized by the slope of origin line used for determination of J_{Qd}^{app}; point of unstable crack growth is intersection between origin line and $J - T_J$-curve.

$$J_d^{app} = \beta_J T_{Jd} \tag{6}$$

where β_J is the material specific parameter.

The slope of this linear function, β_J, is determined by the position of the unstable value of J ("instability point") on the $J - T_J$-curve. For the PP material shown in Figure 1 the value of β_J is $\beta_J = 2.2$. Generally, values were found for β_J between 0.1 to 31.[4] With such $J - T_J$-stability-assessment diagrams the possibility for the unstable toughness characterization in the whole range of temperature and composition is given independent of the crack growth process.

Additionally, the investigated materials were characterized by:

1. dynamic mechanical analysis (DMA), to determine the glass transition temperature, T_g, of the amorphous PP phase and EPR rubber,
2. differential scanning calorimetry (DSC), to detect the crystallinity and the crystallization temperature,
3. further mechanical tests, to determine the flexural modulus and the notched Charpy impact strength of the materials,
4. transmission electron microscopy, to analyze the morphology of the materials (interparticle distance A, particle diameter D). The microtomed ultrathin sections were stained with rutheniumtetroxide (RuO_4) vapor.

Materials

For the investigations, two different PP/EPR copolymers (heterophasic ethylene–propylene random copolymers—RAHECO®[13]) were used, which are designated as material 1 and material 2. The matrix material of material 1 is an ethylene–propylene random copolymer with 4 mol % ethylene in the propylene chain. The ethylene–propylene–rubber (EPR) particles are core shell particles with a PE lamellae core and an EPR shell.

Material 2 is also a combination of an ethylene–propylene random copolymer and EPR particles, but with 8 mol % ethylene in the propylene chain. The EPR particles contain up to 5 crystalline PE inclusions. The particles are smaller and finer dispersed than in material 1.

Both basic materials were melt compounded with the matrix material to lower particle concentrations in a single-screw extruder. The random copolymers used for the dilution were ethylene–propylene copolymers with comparable molecular structures as the matrix materials. The specimens were produced by injection moulding.

RESULTS AND DISCUSSION

Basic Characterization

Mechanical and thermal behavior as well as the characteristic material parameters are given in Tables I and II.

The phase separation during copolymerization is indicated by separately detected tan δ peaks of PP and EPR glass transitions. The PP glass transition temperature of 1°C (material 1) respectively −5°C (material 2) is not affected by blending processes. In contrast to that, a T_g shift of EPR for material 2 was observed.

For the description of the mechanical behavior, the flexural modulus E_f, the flexural strength at peripheral strain of 3.5% according to DIN 43453,[14] and the Charpy impact strength a_{cN} of notched specimens according to ISO 179[15] were used. Whereas the flexural modulus and the flexural strength decrease with increasing RAHECO® content, the Charpy impact strength of both materials increase with increasing RAHECO® content. In the range from 30 to 65 wt % the toughness of material 2 increases rapidly, and above 65 wt % it is nearly constant.

Morphology

Adjustment of matrix and elastomer viscosity in combination with random copolymerization of PP with ethylene, which decreases the surface tension between the two phases, realizes a very fine morphology of the materials.

Table I

Composition $\phi_{RAHECO}/\phi_{Matrix}$ (wt %)	Glass Transition Temperature of EPR T_G(°C)	Crystallization Temperature T_c(°C)	Flexural		a_{cN}(+23°C) kJ/m^2
			Modulus E_f(MPa)	Strength σ_{fc}(MPa)	
100/0	−51.4	110	586	15.3	19.5
90/10	−52.0	111	589	15.4	16.3
80/20	−51.7	109	641	16.8	14.7
65/35	−52.8	109	686	18.2	11.4
50/50	−52.2	108	745	19.7	9.8
35/65	−53.8	108	798	21.3	8.1
20/80	−54.3	107	861	23.0	6.6
10/90	−52.2	106	899	24.2	6.3
0/100	—	104	1009	27.1	4.8

Figure 2 shows the average interparticle distance and the average particle diameter for both materials. For material 1, the average interparticle distance decreases from 4.7 μm at 10 wt % RAHECO® to 1.2 μm at 100 wt % RAHECO® [Fig. 2(a)]. Material 2 shows also a decrease of average interparticle distance with increasing RAHECO® content from 2.2 to 0.36 μm [Fig. 2(a)]. The average particle diameter is nearly constant for material 2. For material 1, an increase of particle diameter from 0.5 to 0.9 μm with increasing RAHECO® content was observed [Fig. 2(b)].

The elastomer particles are well dispersed in the matrix in both materials, as illustrated in the TEMs (Fig. 3). In the micrographs, the particles appear dark owing to staining with RuO_4. Material 1 shows approximately a core shell structure. The higher magnification represents the internal structure of EPR/PE particles. The PE inclusion is surrounded by a dark shell of EPR, which provides to a good adhesion between the matrix and modifier particle [Fig. 3(a)].

At 100 wt % RAHECO® the particles in material 2 are smaller and finer dispersed than in material 1. The internal structure of the particles consist of up to five PE-rich inclusions, which are not clearly separated from each other. Within the inclusions, single PE lamellae exist. The PE-rich inclusions are surrounded by a dark amorphous shell of EPR also [Fig. 3(b)].

Fracture Mechanics Tests

The crack-resistance values against unstable crack growth J_{Id}^{ST} and the approximated values J_{Qd}^{app} in dependence on interparticle distance and test temperature ($-20°C \leq T \leq 40°C$) for material 1 are given in Figure 4. For temperatures above $T = 23°C$, a very strong rise of toughness properties can be observed. The dependencies in

Table II

Composition $\phi_{RAHECO}/\phi_{Matrix}$ (wt %)	Glass Transition Temperature of EPR T_G(°C)	Crystallization Temperature T_c(°C)	Flexural		a_{cN}(+23°C) kJ/m^2
			Modulus E_f(MPa)	Strength σ_{fc}(MPa)	
100/0	−47.1	98.8	329	8.9	69
90/10	−46.8	98.8	363	9.9	70.6
80/20	−47.6	98.5	401	10.8	70.3
65/35	−49.9	97.3	459	12.5	68.4
50/50	−51.3	97.7	514	14.1	54.6
35/65	−51.8	97.2	583	16	16.6
20/80	−54.4	96.5	652	17.8	11.4
10/90	−55.0	96.2	697	19.1	9.4
0/100	—	94.3	730	21.9	7.6

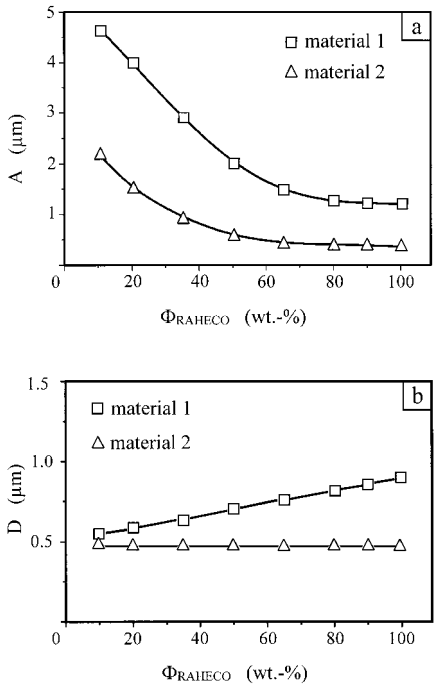

Figure 2 Average interparticle distance, A (a), and average particle diameter, D (b), in dependence on RAHECO®-content of material 1 and material 2.

Figure 4(a) explain that the determination of quantitative dependencies of crack-resistance values against unstable crack growth with conventional experimental fracture mechanics values (J_{Id}^{ST}) is impossible due to a change in the dominant crack growth mechanism from unstable to stable. In the stable region no specimen fracture occurs (for instance, at $T = 23°C$ and interparticle distances of $A \leq 1.4$ µm), and therefore, no J_{Id}^{ST} values can be determined.

With increasing test temperature the brittle-to-tough transition shifts to higher interparticle distances and critical interparticle distances can be determined. The strong increase in toughness above the critical interparticle distance cannot only be reduced on the influence of temperature but also highly on the influence of the structure.

The critical interparticle distance increases strongly with temperature, and is independent of glass transition temperature of PP [Fig. 4(b)]. Based on the experimental data from all test temperatures it is possible to describe this correlation with an empirical equation [Fig. 4(b)]. These values of the critical interparticle distance, A_c, are independent of specimen geometry, specimen dimensions, and the applied experimental method. For that reason, the values can be understood as intrinsic material parameters.

The results for material 2 are shown in Figure 5. Here, a similar material behavior can be proven. The toughness increasing at $T = 23°C$ is much higher than in material 1. A linear dependence between A_c and test temperature was found also.[16] Differences between the constants of the linear fits should be influenced by molecular parameters of the different matrix materials and different particle structures. For specification of these empirical constants the temperature dependencies of brittle-to-tough transitions of several polymer blends based on different materials as well as materials with distinctive morphologies have to be investigated.

From the temperature dependence of J_{Id}^{ST} it becomes clear that the mechanical behavior changes in a characteristic manner. Typical load (F)–deflection (f) curves of materials with different interparticle distances are shown in Figure 6. In the materials, two transitions in the load–deflection behavior can be observed. A sharp notched PP specimen exhibits brittle failure un-

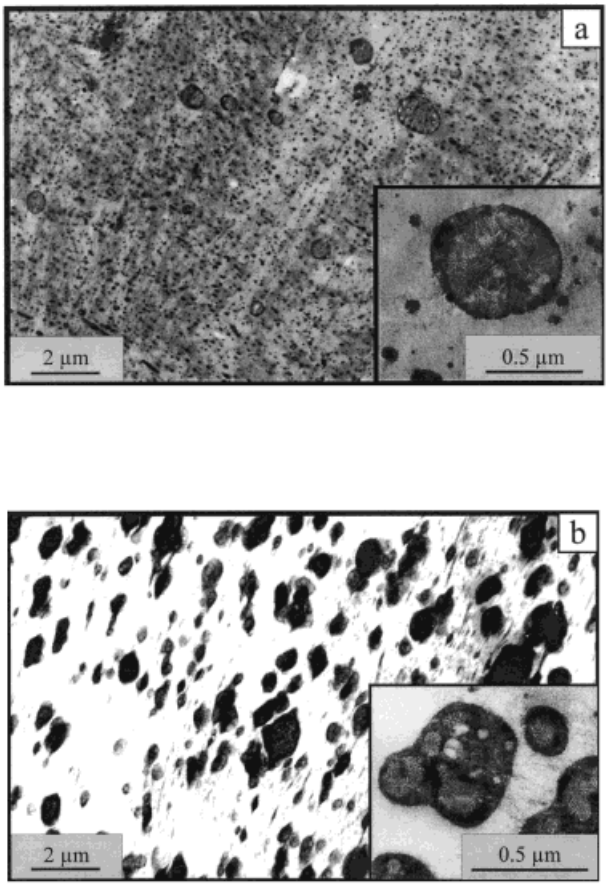

Figure 3 TEMs of particle distribution and internal structure of EPR/PE particles of material 1 (a) and material 2 (b) at different magnifications.

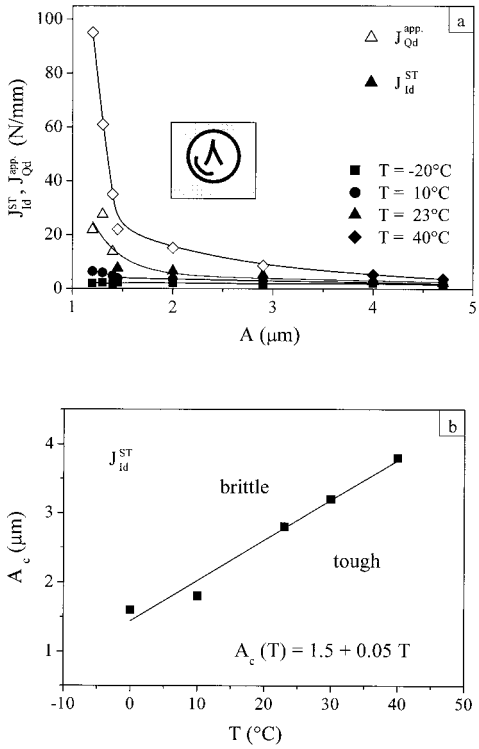

Figure 4 Influence of particle distance on the critical J_{Id}^{ST}- and J_{Qd}^{app}-values (a) and critical interparticle distance A_c for the brittle-to-tough transition of material 1 vs. temperature (b).

der impact conditions. The material behavior can be characterized as linear–elastic. The first transition occurs from pure elastic (a, b) to elastic–plastic material behavior with decreasing interparticle distance (c). In both cases the materials break in a brittle manner. The crack growth is predominant unstable. The second transition to predominantly stable crack growth without specimen fracture is characterized by a large increase in toughness, and the brittle-to-tough transition can be determined. At the end of this process only stable crack growth without specimen fracture occurs [Fig. 6(d)]. All materials with such load–deflection behavior are not considered by the determination of critical interparticle distances (Figs. 4 and 5).

The determination of fracture mechanics values as resistance against stable crack growth requires the determination of the correlation between a fracture mechanics loading parameter and the stable crack growth, Δa. The concepts of yield fracture mechanics (i.e., J-Integral and COD concept) are well established for the determination of the loading parameters in the case of elastic–plastic material behavior. Between the limits of J, respectively, δ-controlled stable crack growth, the J_R, respectively, δ_R curves, characterize the crack resistance in the ductile failure area. By that, it is possible to quantify the stages of stable crack growth process: crack tip blunting, crack initiation, and stable crack growth.

The experimental investigations about the influence of the test methods[4,5] for determination of dynamic crack resistance curves show that the multiple specimen stop-block technique is the experimental basis for a reproducible determination of the fracture mechanics values.

The J_R curves of material 1 at $T = 30°C$ for different interparticle distances are given in Figure 7. With decreasing interparticle distance an obviously increasing of the technical crack initiation values ($J_{0.2}$) as well as the tearing modulus T_J can be proven. In the right part of Figure 7 the $J_{0.2}$ values as a function of the interparticle distance at $T = 30°C$ are shown. The crack initiation values show a strong decreasing in dependence on interparticle distance between 1.2 and 1.5 μm, and the determination of a critical interparticle distance at $A_c = 1.4$ μm is possible.

On principle, the dependencies $J_{0.2} = f(A)$ and $J_{Id}^{ST} = f(A)$ show a similar behavior. That means two transitions occur—one in the region of predominant unstable crack growth, and a second in the region of predominant stable crack growth.

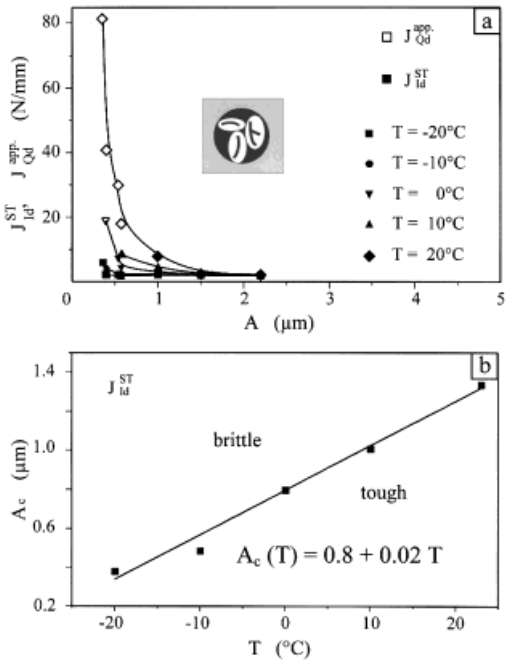

Figure 5 Influence of particle distance on the critical J_{Id}^{ST}- and J_{Qd}^{app}-values (a) and critical interparticle distance A_c for the brittle-to-tough transition of material 2 vs. temperature (b).

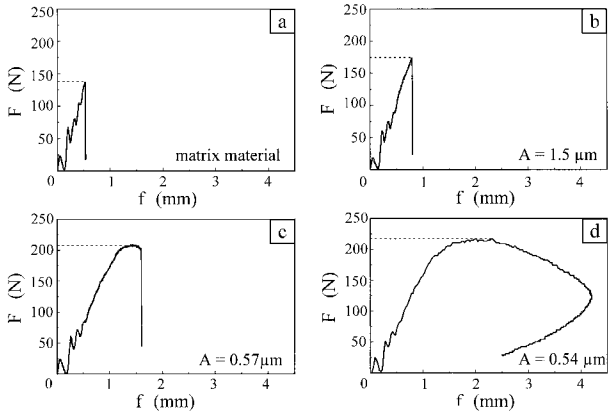

Figure 6 Load (F)–deflection (f) curves of selected materials recorded with the instrumented Charpy impact test (material 2).

This second value is clearly smaller than the value in the region of unstable crack growth. Below both "critical interparticle distances" a characteristic increasing of toughness values occurs.

SEM observations (Fig. 8) show that cavitation is the main deformation mechanism in these materials below the second "critical interparticle distance." The materials differ only in the number of cavities; that means in the intensity of the cavitation process [Fig. 8(a), predominant unstable crack growth below first "critical interparticle distance"; Fig. 8(b), predominant stable crack growth in the region of second "critical interparticle distance"]. A further decreasing of interparticle distance results in an overlapping of cavitation and fibrillation processes [Fig. 8(c), above a second "critical interparticle distance"]. The quantity as well as the quality of the deformation process changes. The cavitation process itself can

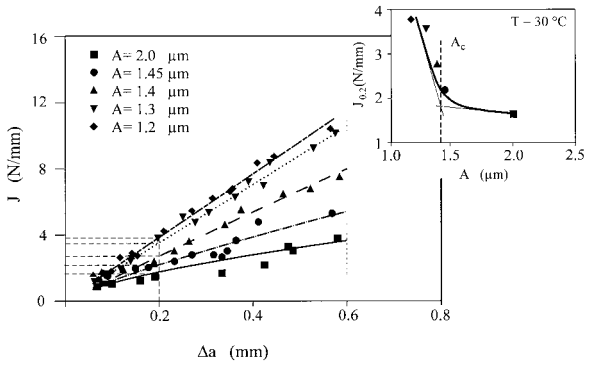

Figure 7 J_R curves of material 1 (T = 30°C) and technical initiation values, $J_{0.2}$ vs. average interparticle distance A.

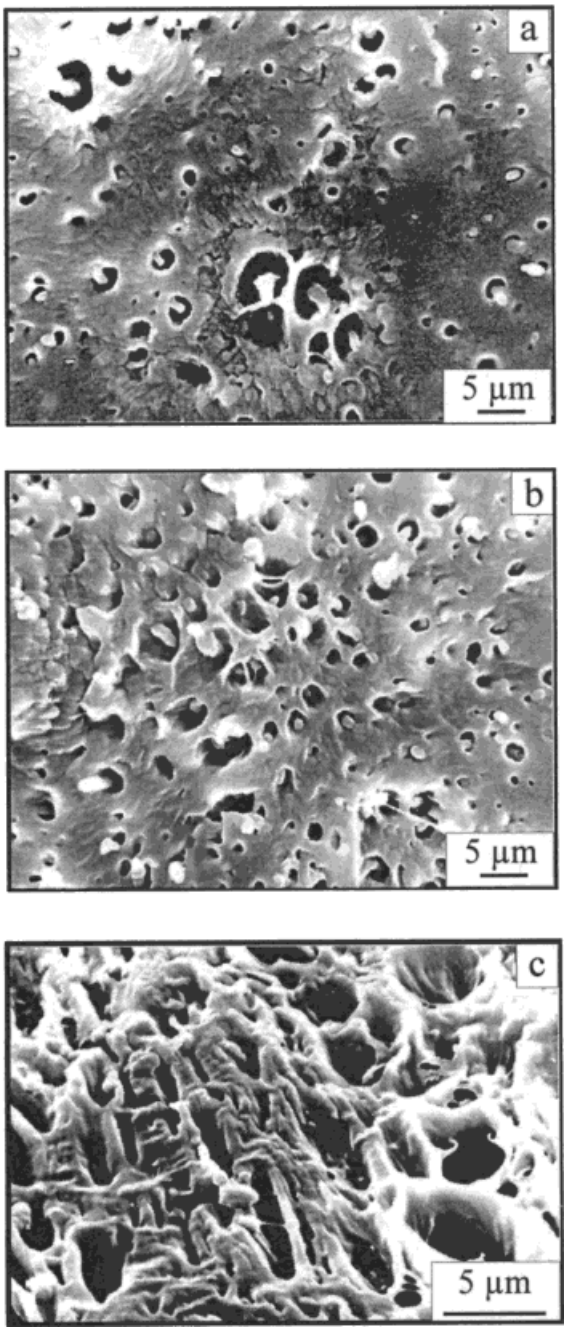

Figure 8 SEMs of material 1. (a) Cavitation in the damage zone, unstable crack growth, average interparticle distance A = 2.9 μm; (b) cavitation in the region of stable crack growth, average interparticle distance A = 1.4 μm; (c) cavitation and fibrillation in the region of stable crack growth, average interparticle distance A = 1.3 μm.

be reduced to deformation processes in the EPR shell or on the interface EPR/PE, respectively.

Material 2 shows comparably results (Fig. 9). With decreasing interparticle distances technical

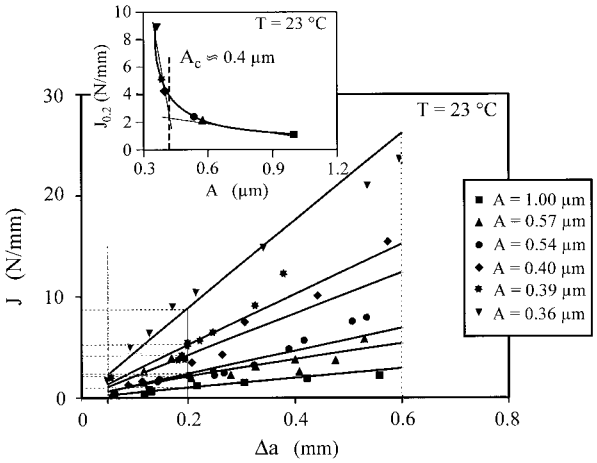

Figure 9 J_R curves of material 2 (T = 23°C) and technical initiation values, $J_{0.2}$, vs. average interparticle distance A.

initiation values and tearing modulus increase, and a second "critical interparticle distance" can be determined also. The calculated value ($A_c \approx 0.4$ μm) is clearly smaller than the value in the region of the unstable crack growth.

The effect of a second "critical interparticle distance" presented as tough-to-high impact transition was found in other PP blends at different test temperatures.[4,17]

On the basis of the different crack growth mechanisms and, therefore, on the basis of different fracture mechanics values a brittle-to-tough and a tough-to-high impact transition can be proven. For a direct comparison of both materials it is necessary to use the $(A/D)_c$ (critical interparticle distance to particle diameter) ratio. Figure 10 shows the $(A/D)_c$ in dependence on temperature for both materials. The two characteristic dependencies in the region of predominant unstable crack growth and in the region of predominant stable crack growth are represented. In both materials a stronger dependence on temperature for the unstable than for the stable crack initiation values can be proven. On the basis of the results given in Figure 10, two additional effects are evident: (a) In material 2, toughness increasing starts above the glass transition temperature of the EPR, and in material 1 above the glass transition temperature of the PP. Altogether, the toughness increasing in material 2 is much higher than in material 1. (b) To change the predominant crack growth mechanism from unstable to stable in the more brittle material (material 1) a stronger reduction of interparticle distance is necessary than in the tougher material (material 2). That means the differences between these values become larger.

The toughness optimization in the region between the glass transition temperatures of the EPR and the PP, i.e., low-temperature toughness, requires an adjustment of particle diameter and interparticle distance to matrix material.

The results of the fracture mechanics tests indicate a validity of Wu's percolation theory[1] if predominant unstable fracture occurs. In the region of predominant stable crack growth, the theory by Margolina et al.[3] is valid. This theory is based on the consideration that changes from plane strain to plane stress conditions in thinner matrix ligaments (i.e., with decreasing interparticle distance) reduces the critical stress for matrix yielding.

In both theories[1,3] the matrix deformation processes are primarily considered. As can be proven, for example, in ref. 16, the particles play a decisive role in the deformation process. Therefore, it is necessary to include the deformation processes of the particles in the discussion. These considerations must be specified, and their validity must be checked on other materials.

CONCLUSIONS

1. Heterophasic reactor-grade propylene–ethylene copolymers were diluted with a matrix-like propylene–ethylene random copolymer to obtain materials with constant particle diameter but various interparticle distances.
2. Based on optimized test conditions, it is

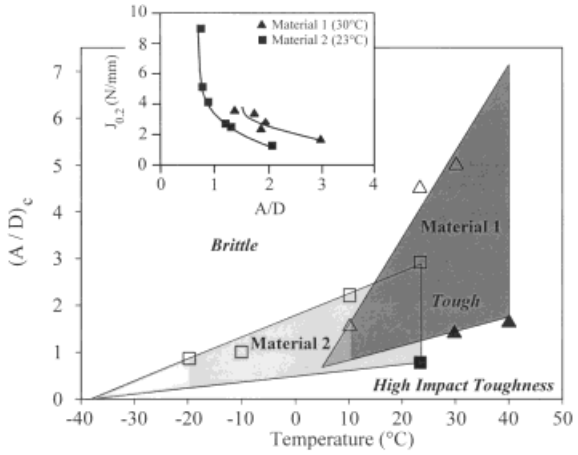

Figure 10 Dependence of critical ratio $(A/D)_c$ (interparticle distance to particle diameter) on temperature in the region of stable and unstable crack growth.

possible to determine geometry-independent fracture mechanics values as resistance against unstable and stable crack growth. These intrinsic values enable a micromechanical interpretation of toughness mechanisms.

3. The application of a new technique, called "$J - T_J$-stability-assessment diagrams", allows the description of toughness dependencies on temperature.
4. The crack-resistance behavior is strongly affected by the critical interparticle distances and the temperature. Critical interparticle distances can be determined in the region of predominant unstable crack growth as well as in the region of predominant stable crack growth.
5. With increasing temperature, the brittle-to-tough transition in the region of unstable crack growth shifts to higher interparticle distance, and can be described with an empirical equation.
6. The toughness characterization in the region of predominant stable crack growth requires the determination of crack resistance curves. The structural parameters of morphology, like interparticle distance or $(A/D)_c$ ratio, have a stronger influence on crack growth behavior than on the crack initiation behavior.

OUTLOOK

For fracture toughness optimization of polymers and evaluation of structural integrity assessment of components the fracture mechanics of polymers has been intensively researched during the past years with the aim to develop the field application of fracture mechanics values. Several fracture mechanical parameters have been proposed for the evaluation of the crack-resistance behavior. In the first step, until 1985, the determination of fracture mechanical behavior was accomplished on the basis of the LEFM and EPFM concepts, and fracture mechanics values against unstable crack growth were determined.[4] In the second level, the fracture–mechanical assessment was accomplished on the basis of the J_R-integral curves. On this level, all scientists work currently all over the world. The quantitative integration of the crack growth behavior is indispensable for an effective application of the fracture mechanics values on materials development. Only a few works consider the time dependence of the fracture mechanical assessment. A quantity of instinct and spirit is necessary to obtain an improvement and a rise of knowledge in the upcoming years.

The authors would like to thank German Research Council (DFG) for the financial support of this study which forms part of research programme "Innovationskolleg: New Polymeric Materials." They also thank Dr. M. Gahleitner, Mr. J. Fiebig, and Mr. C. Paulik at Borealis AG, Linz, Austria, for supplying the materials and many interesting discussions.

REFERENCES

1. Wu, S. Polymer 1985, 26, 1855.
2. Borggreve, R. J. M.; Gaymans, R. J.; Luttmer, A. R. Makromol Chem Macromol Symp 1988, 16, 195.
3. Margolina, A. Polym Commun 1990, 31, 95.
4. Grellmann, W.; Seidler, S., Eds. Deformation and Fracture Behaviour of Polymers; Springer Verlag: New York, 2001.
5. Seidler, S.; Grellmann, W. Polym Testing 1995, 14, 453.
6. Grellmann, W.; Sommer, J.-P. Fract Mech Micromech Coupled Fields (FMC)-Series 1986, 17, 48.
7. Sumpter, J. D.; Turner, C. E. Intern J Fracture 1973, 9, 320.
8. DIN EN ISO 178. Plastics—Determination of Flexural Properties, 1996.
9. Savadori, A.; Bramuzzo, M.; Marega, C. Polym Testing 1984, 4, 73.
10. Seidler, S. Fortschrittberichte VDI-Reihe 18: Mechanik/Bruchmechanik; VDI-Verlag: Düsseldorf, 1998, 231, Vol 97.
11. Grellmann, W.; Seivler, S. In Winkler, T.; Schubert, A., Eds., Mater Mech Fracture Mech Micromech DDP Goldenberg Dresden (Germany) 1999, 336.
12. Paris, P. C.; Johnson, R. E. ASTM STP 803 1983, II, 5.
13. Paulik, C. Kunststoffe 1996, 86, 1144.
14. DIN 53453. Schlagbiegeversuch an Probekörpern ohne oder mit U-Kerb, 1982.
15. ISO 179. Plastics—Determination of Impact Strength, 1996.
16. Starke, J. U.; Michler, G. H.; Grellmann, W.; Seidler, S.; Gahleitner, M.; Fiebig, J.; Nezbedova, E. Polymer 1998, 39, 75.
17. Seidler, S.; Grellmann, W. In Kahovec, I., Ed., Mechanical Behaviour of Polymeric Materials. Wiley-VHC Weinheim, 1999, 63.